Deterministic chaos in the elastic pendulum: A simple laboratory for nonlinear dynamics

R. Cuerno, A. F. Rañada, and J. J. Ruiz-Lorenzo

Instituto de Física Fundamental y Departamento de Física Teórica I., Facultad de Ciencias Físicas, Universidad Complutense, 28040 Madrid, Spain

The chaotic motion of the elastic pendulum is studied by means of four indicators, the Poincaré section, the maximum Lyapunov exponent, the correlation function, and the power spectrum. It is shown that for very low and very large energies the motion is regular while it is very irregular for intermediate energies. Analytical considerations and graphical representations concerning the applicability of KAM theorem are also presented. This system and the type of description used are very suitable to introduce undergraduate students to nonlinear dynamics.

I. INTRODUCTION

The elastic pendulum, although rather a simple mechanical system, combines a complex dynamical behavior with a wide applicability as a mathematical model in different fields of physics, such as nonlinear optics or plasma physics.[1] The techniques used to tackle this simple but at the time complex system range from perturbative studies (where parametric resonance has been found, due to the existence of energy transfer among the different modes)[1-3] to experimental studies that use stroboscopic techniques.[4] In any case it is clear that such an apparently uninteresting system with just 2 degrees of freedom displays a rich and varied dynamics. A method that is complementary to the above mentioned, and which has been widely used in the literature for other dynamical systems, is the numerical computation of several indicators able to characterize the kind of evolution one has for each set of parameters and initial conditions. However, each indicator alone can be misleading. We shall see later that the joint use of several indicators may greatly clarify the analysis of the evolution. Our system displays one kind of motion for a range of parameters, and a drastically different motion for other values. This feature enables us to compare the efficiency of standard methods in the numerical characterization of chaos.

We consider a Hamiltonian system, with N degrees of freedom, to be chaotic when the maximum number of dynamical variables in involution (i.e., with Poisson brackets equal to zero) is less than the number of degrees of freedom N. This is because an important theorem due to Liouville[5,6] states that when there are N conserved quantities in involution the solution of the equations of motion can be obtained by quadratures and the behavior is regular. Moreover, it is observed that when this is not the case the system behaves stochastically, at least some of the solutions being unstable.

As it is not easy to prove that there are no such quantities, one has to resort to some indicators, four of which are studied in this paper. We will admit that there is chaos if several of these indicators show this to be the case.

In the next section we shall briefly describe our system. We will stress the lack of a sufficient number of conserved quantities for the system to be exactly solved. Then we consider some formal arguments at high and low energy regimes, which may explain numerically observed behaviors. They will tell us about the exact integrability of the system at those particular regimes. The applicability of the KAM theorem will also be examined and consistency with numerical results will be checked. In the third section the main results of the paper are presented. We characterize the motion by use of four different numerical indicators (Poincaré section, maximum Lyapunov exponent, correlation function, and power spectrum). This is done for examples of both regular and irregular types of motion. Finally, some conclusions are presented.

II. EQUATIONS OF MOTION

The Lagrangian of the plane elastic pendulum, in the Cartesian coordinates of Fig. 1, is

$$L = m(\dot{x}^2 + \dot{y}^2)/2 - mgy - (k/2)[(x^2 + y^2)^{1/2} - l_0]^2, \tag{1}$$

where no approximation has been made; l_0 is the natural length of the pendulum, k is the spring elastic constant, m is the mass of the bob, and g is the gravitational acceleration on the Earth surface. The Euler–Lagrange equations of motion are

$$\ddot{x} = -\omega_s^2 x + g\lambda x/(x^2 + y^2)^{1/2}, \tag{2}$$

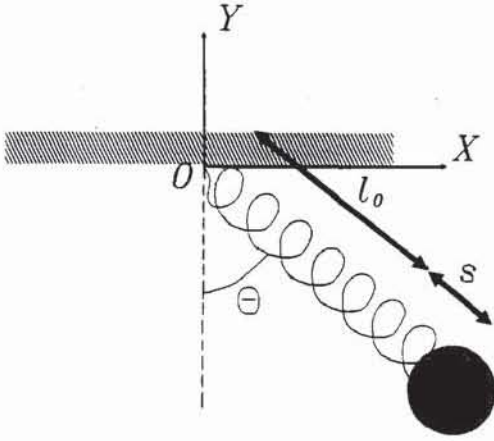$$\ddot{y} = -g - y\omega_s^2 + g\lambda y/(x^2 + y^2)^{1/2}, \tag{3}$$

Fig. 1. The elastic pendulum.

where we have defined $\omega_s^2 \equiv k/m, \omega_p^2 \equiv g/l_0$, $\lambda \equiv \omega_s^2/\omega_p^2$, and $\lambda, \omega_p, \omega_s$ are positive. The principal feature of these equations is the nonlinear coupling between the vertical and horizontal motions. As a limiting case one can easily see that if $\theta \ll 1$ and $s \ll l_0$ one is left with two decoupled oscillators of very simple behavior, where θ is the angle with the vertical and s is the deformation of the spring (see Fig. 1).

One conserved quantity (it does not change in the temporal evolution) is the energy of the system (E):

$$\frac{E}{m} = \frac{\dot{x}^2 + \dot{y}^2}{2} + gy + \frac{\omega_s^2}{2}[(x^2 + y^2)^{1/2} - l_0]^2. \quad (4)$$

The number of conserved quantities is very important because of the Liouville theorem.[5,6] By this theorem we know that a mechanical system of N degrees of freedom is integrable if there exist N independent conserved quantities of motion such that their Poisson brackets are equal to zero (in this case they are said to be in involution). Moreover, the theorem implies that the phase space is formed by hypertori (tori of N dimensions) and that all the trajectories remain on their hypersurfaces (see Fig. 2). This figure is for a system with 2 degrees of freedom. There are two natural frequencies, which are $\dot{\varphi}_1, \dot{\varphi}_2$, where φ_1 and φ_2 are angle variables (see the definition in Fig. 2). If the Liouville theorem conditions hold, the motion will be regular; otherwise some tori in the phase space disappear, which implies nonintegrability. This is because, in this case, there are not enough conserved quantities and the trajectories are not classified in an N-dimensional hypersurface. As a
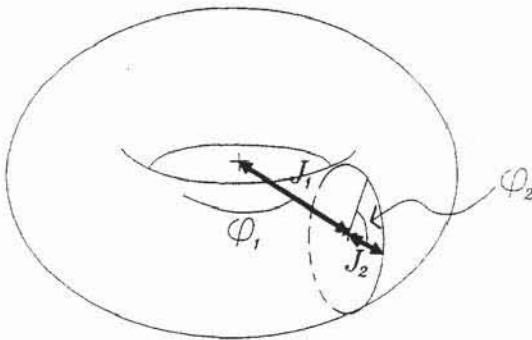

Fig. 2. Angle action variables on a two-dimensional torus.

consequence, they fill regions of the phase space with more than N dimensions and the behavior becomes much more complex.[5] For our system, integrability would need a new conservation law (or conserved quantity), which would be independent of the energy. Known results[1-4] (confirmed by our data) show that such a conservation law does not exist. This is usually understood as implying that the equations of motion cannot be solved by quadratures,[5] a property that we take as a sufficient condition for complex behavior.

III. ANALYTICAL RESULTS

The motivation of this section is to show the integrability of the system for some limiting cases related with large values of $|E/m|$, whereas for intermediate values one has both regular and irregular trajectories in phase space. This has also been reported elsewhere.[1] Analytical considerations and graphical representations concerning the KAM theorem are also presented.

A. Low and high energy limits

There are several limits of the parameters, and, through these, of the energy, in which the system turns out to be integrable. A possibility we can consider is taking the limit $E/m \to \infty$. In order to get large positive values of E/m we shall start from the expression for the Lagrangian in the polar coordinates of Fig. 1:

$$L = (m/2)(\dot{r}^2 + r^2\dot{\theta}^2) + mgr\cos\theta - (k/2)(r - l_0)^2. \quad (5)$$

If the energy is large, either r is large, or the kinetic energy is. In the former case $mgr\cos\theta$ can be neglected, and one is left with a separable Lagrangian (i.e., integrable system). In the latter $(r \sim l_0)$ the kinetic term dominates and the particle moves freely, again an integrable case.

A condition for the energy limit $E/m \to -\infty$ to hold is that $g \to \infty$ [see (4)]. In this limit the equations of motion become (we assume that $x/y \sim 0$ for the deduction of the following formulas):

$$\ddot{x} = -\omega_s^2 x, \quad (6)$$

$$\ddot{y} = -g - l_0\omega_s^2 - \omega_s^2 y. \quad (7)$$

For a given initial condition, because g is large, $x/y \sim 0$ according to the assumptions. Furthermore, the system becomes equivalent to two uncoupled linear oscillators (x and y coordinates), i.e., again an integrable system.

These qualitative arguments agree with the conclusions of some other references.[1]

B. KAM theorem applicability

The KAM theorem[6] tells us essentially, in the case of two degrees of freedom, that if we add a perturbation to an integrable system:

$$H = H_0 + \epsilon H_1 \quad (8)$$

(where H_0 is an integrable Hamiltonian, H_1 is a conservative perturbation, and ϵ is the perturbation parameter), some of the tori will only be distorted (but not destroyed), the measure of which being determined by the value of ϵ. Moreover, this measure decreases as ϵ grows. The conserved tori are those for which the frequency rate $\dot{\varphi}_1/\dot{\varphi}_2$ is sufficiently irrational[5] (i.e., it cannot be approximated by rational numbers better than a bound essentially dictated

by the size of the perturbation). As for the tori which do not satisfy this condition, they disappear and are replaced by chaotic layers in which the trajectories explore three-dimensional regions in phase space, the tori being two dimensional.[5,7,8] What happens is that the behavior of the system becomes more complex as the number of conserved tori decreases and the size of the chaotic layers grows when ϵ increases.

The conditions of applicability of this theorem are that the original system be conservative, nondegenerate [a functional relation such as $\omega_1 = f(\omega_2)$ does not exist] and isoenergetically nondegenerate (the derivative of the rate of frequencies with respect to the action variables is non-zero).[5,6]

As a first approximation we could consider the nonperturbed Hamiltonian as a sum of the spring and pendulum Hamiltonians. But this system is degenerate, since the frequency ratio (ω_p/ω_s) is constant for all the tori. To avoid this problem we start with the complete Hamiltonian:

$$H = 1/(2m)(p_x^2 + p_y^2) + mgy + (1/2)k\,[(x^2 + y^2)^{1/2} - l_0]^2, \qquad (9)$$

which we decompose in the following way:

$$H_0 = 1/(2m)(p_x^2 + p_y^2) + \lambda mg/l_0^3(y'^4 + 1/4x^4), \quad (10)$$

where we have defined $y' \equiv y + l_0$. H_0 is integrable since it is separable, and we will take

$$V_P \equiv H - H_0, \qquad (11)$$

where V_P will play the role of ϵH_1 in (8). The action variables (see Ref. 9) for the Hamiltonian (9) turn out to define frequencies which verify the KAM conditions, with the decomposition (11). In addition to the explicit computation, one can see that H_0 is the sum of two anharmonic oscillators, for which the period is amplitude dependent, and this could justify the functional independence of the two frequencies, i.e., the fulfillment of the KAM requirements.

H_0 may be seen as the resulting term that emerges from H when the condition $|y| \ll |x| \ll l_0$ is assumed (this is a physical justification of the otherwise mathematically valid previous decomposition). The corresponding expression for V_P is

$$V_P = mgy' - mgl_0 + \lambda mg/l_0^3(-y'^2x^2) + \text{higher orders.} \qquad (12)$$

We can take ϵ in (8) as λ but in doing so we have that H_0 depends on ϵ and in principle KAM theorem may not be applied, *but* since H_0 is integrable from all λ (its phase space is qualitatively as that of an H_0 which were independent of any perturbation parameter at all) and fulfills all the KAM requirements, the phase space of the complete Hamiltonian (9) is just as that predicted by KAM theorem for a perturbed Hamiltonian (8) and this for all values of λ.

In Fig. 3 one can see the coexistence of broken and unbroken tori described by the KAM theorem. The energy increases from Fig. 3(a)–(c) and we can see that the effect of this is an increase of the region occupied by chaotic trajectories, i.e., broken tori.

IV. NUMERICAL RESULTS

There are, roughly speaking, two techniques for the study of a nonlinear problem: perturbative and numerical methods. A virtue of the numerical methods is that they
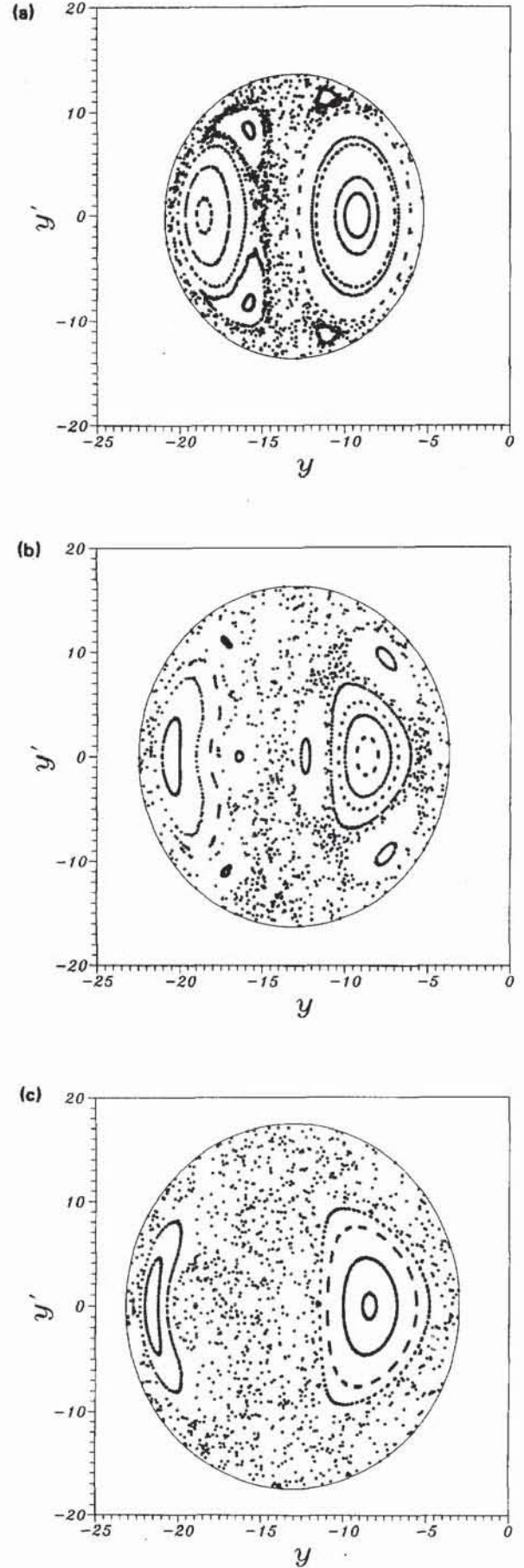

Fig. 3. Poncairé sections for different values of the energy: $E/m = -20$ J/kg for (a), $E/m = 20$ J/kg for (b) and $E/m = 40$ J/kg for (c). In all three cases $\omega_m^2 = 3\,\text{s}^{-1}$, $\lambda = 3$. In every case the continuous curve marks the boundary of the energetically allowed region on the surface of section.

deal with the complete equations, without extra assumptions. The possibility of displaying graphically certain parameters, which distinguish between regular and chaotic motion adds to this option a large pedagogical interest. Some computations can be made with the aid of a compatible PC, but others must be done on a main frame (e.g., IBM 4381 or IBM 3090, as for our case).

The calculations of our parameters (Lyapunov exponent, Poincaré section, correlation function, and power spectrum) are based on numerical integration of the Euler–Lagrange equations, which was performed using a fourth-order Runge–Kutta method and a predictor-corrector like that of Milne.[10] In the numerical integration we have checked that the conservation of the energy still holds for the discretized system. Other researchers[11] have verified that all the trajectories remain in their respective energy hypersurface, even the chaotic ones. We have also verified this fact in our work.

In numerical experiments analysis of computational errors is needed. In general there are two different kinds of errors: round-off (due to the computing device) and truncation (due to the nature of the numerical methods) errors. Control on these errors has been achieved by the change of the step in the numerical integration. It can be shown that in the fourth-order Runge–Kutta method:[10]

$$c \equiv [x_h(t_f) - x_{h/4}(t_f)]/[x_{h/2}(t_f) - x_{h/4}(t_f)]$$
$$= 2^4 = 16, \qquad (13)$$

where h is original step of numerical method, t_f is the final value of the independent variable, and $c = 16$ because the truncation error is proportional to h^4, if we ignore the round-off errors. Therefore, we will have a non-negligible round-off error when our computed value for c is different from 16. It is still acceptable for a value of c between 8 and 32, say. A different kind of test has been the numerical inverse integration, that is, we have integrated the equations backwards, taking some point as an initial condition and checking whether we recovered the primitive one. Moreover, two numerical schemes of different nature in their construction (Runge–Kutta and Milne methods) have been used for the computations, with the aim of controlling eventual instabilities.

A. Poincaré map

This procedure starts with the choice of a value for the energy (and of course all the other parameters of the system). This reduces the number of independent coordinates for our system from four $(x,y,\dot{x},\dot{y})$ to three (i.e., $y, \dot{x},\dot{y}$). If an independent conserved quantity other than the energy exists, this would reduce the number of independent variables to two. In this case if we take one of the three variables to be constant (x), the points where the trajectory intersects the so-defined plane (with $\dot{x} > 0$) will form a well-defined curve. If such a conserved quantity does not exist, the constraint disappears and the intersection points tend to densely fill this plane which we will call surface of section or Poincaré section. This is the case for chaotic motions. The mapping that takes us from a point on the surface of section to the next one is called a Poincaré map.

This indicator allows a direct visualization of the regularities or irregularities or a given trajectory. It is easier to reliably identify regular than chaotic ones, by the use of this method.
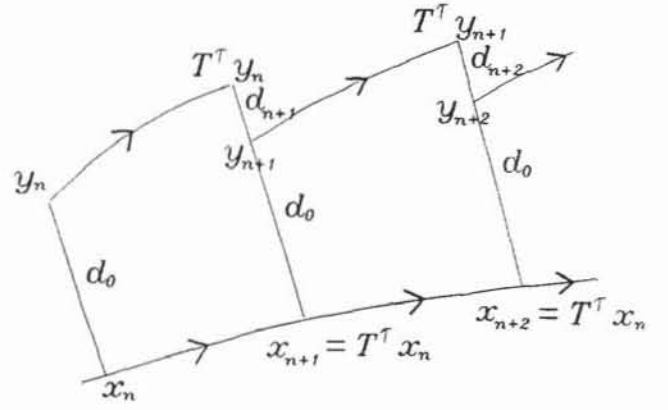

Fig. 4. Schematic description of the maximum Lyapunov exponent numerical computation. d_0 is the fiducial distance between the two nearby initial conditions x_0, y_0. $y_n = T^\tau y_{n-1}$ is the nth point obtained in a numerical integration with time step τ, with initial conditions y_{n-1}.

B. Lyapunov exponent

A defining feature of chaotic systems is the sensitive dependence on initial conditions; this implies that after large time lapses the distance between nearby trajectories grows exponentially as $\exp(\lambda t)$, while such divergence is as t^n for regular systems. In a regular (i.e., nonchaotic) system this divergence can also be exponential if the accessible region of phase space is unbounded, as the example $\dot{x} = x$ with solutions $x = x_0 \exp(t)$ shows. If this region is bounded locally, this exponential separation can only occur during short periods of time. For this region a combination of bounded accessible region of phase space and positive Lyapunov exponent is usually interpreted as an indication of chaotic behavior. The more so since the calculation of this number really gives its average along a trajectory.

To characterize these phenomena we have defined:

$$k_n = \frac{1}{(n\tau)} \sum_{i=1}^{n} \log \frac{d_i}{d_0}, \qquad (14)$$

where $n\tau$ is the total time integration lapse and d_i, d_0 are defined in Fig. 4. The motivation for the definition in the last equation is the search for exponential divergences. It can be shown that

$$K_1 = \lim_{n \to \infty} k_n, \qquad (15)$$

where K_1 is the maximum Lyapunov experiment.

Numerical results[12,13] have suggested that in the chaotic regions of phase space $K_1 > 0$, while in the regular regions $K_1 = 0$. (This because K_1 is then proportional to the limit of $\log t/t$ when $t \to \infty$). Therefore, the maximum Lyapunov exponent is a very good indicator for determining the type of motion one has for a given set of parameters and initial conditions. But one must be aware that it is not possible to rigorously take a limit by numerical means, and one may find a trajectory for which k_n tends to zero, as far as the computer numerical precision is concerned, while actually $K_1 > 0$.

The conclusion is that the maximum Lyapunov exponent is a good indicator for characterizing the trajectories with $k_n > 0$ (i.e., the irregular ones), whenever k_n has a bigger value that of the sum of round-off and truncation errors.

4

C. Correlation function

An important feature of a chaotic trajectory is the non-existence of regularity patterns. During its time evolution the trajectory loses information about its previous history; this fact is described by the values taken by the autocorrelation function C_m. This function tends to zero when the time interval $m\Delta t$ is large; this is for chaotic regimes. Meanwhile, for a regular solution it is generally accepted that the correlation function does not tend to zero.[5,14]

Let $\{x_i\}$ be a discrete signal obtained as the output of the numerical methods used in the resolution of the motion equations. Its correlation is defined as

$$C(m\Delta t) \equiv C_m = \frac{1}{n}\sum_{i=1}^{n} x_i' \cdot x_{i+1}', \qquad (16)$$

where

$$x_j' \equiv x_j - \langle x \rangle, \quad \langle x \rangle \equiv \frac{1}{n}\sum_{i=1}^{n} x_k,$$

Δt is the time step of the numerical method and $n\Delta t$ is the total correlated interval.

If the number of data is large, the limit $n \to \infty$ can be taken, and

$$C_m \simeq \frac{1}{n}\sum_{i=1}^{n} x_i \cdot x_{i+1} - \langle x \rangle^2. \qquad (17)$$

In this way the correlation function indicates the deviation of x_j from its average value, or, more precisely, how much the difference $x_j - \langle x \rangle$ resembles its value for a given time, $m\Delta t$ time units later. Taking the product between both values and summing up to every instant means that if the signal changes only slightly after m steps, C_m will have a considerable value, since all the summands will have the same sign, and this indicates that the signal loses no memory. However, if the signal changes much in this time interval (when taking the limit $n \to \infty$), the sum of products will tend to zero; this will tell us about information loss of the signal and the impossibility of long term predictions.
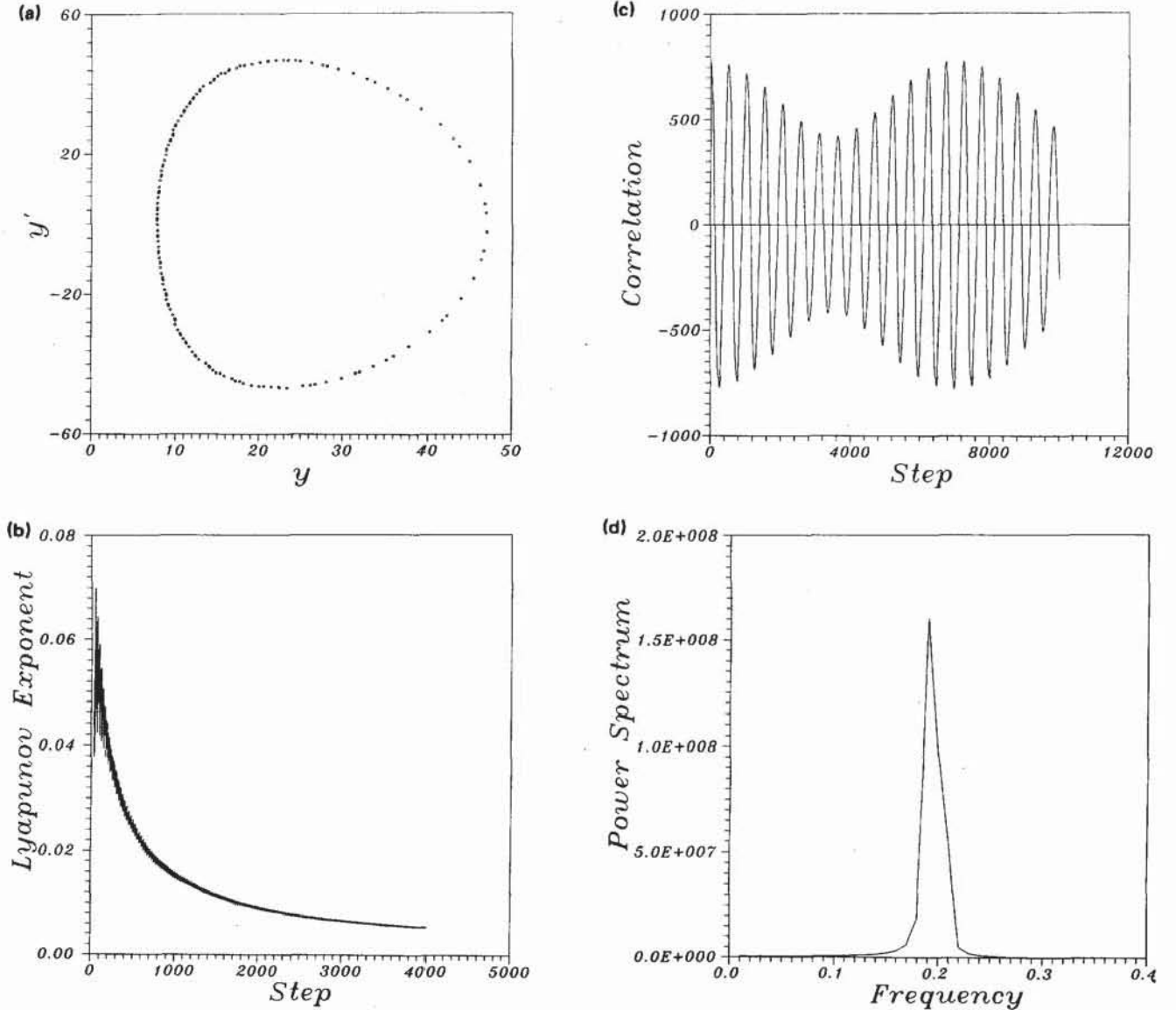

Fig. 5. Plot of several indicators for a trajectory with parameters $E/m = 2000$ J/kg, $\omega_s^2 = 2$ s^{-1}, $\lambda = 2$, and initial conditions $x = y = 10$ m, $\dot{y} = 10$ m/s. In the plot $\dot{y} \equiv y'$. Poincaré section is plotted in (a); the maximum Lyapunov exponent is in (b); correlation function is in (c), and power spectrum is in (d).

5

(There are some instructive examples.[14]) This parameter enables more reliable interpretation for regular behaviors, rather than for chaotic ones, because of the difficulty of demonstrating numerically that a given parameter takes zero value.

D. Power spectrum

A good measure of the patterns of regularity for a signal is provided by Fourier transform. This is defined as follows

$$\tilde{x}_k \equiv \sum_{j=1}^{n} x_j \exp \frac{-2\pi i k j}{n}, \tag{18}$$

where $x_j \equiv x(j\Delta t)$, $\tilde{x}_k \equiv \tilde{x}(k\Delta f)$, $\Delta f \equiv 1/t_{max} = 1/(n\Delta t)$, and Δt is the temporal step. So, the power spectrum is defined as

$$E_k \equiv |\tilde{x}_k|^2. \tag{19}$$

If the signal is periodic, its power spectrum gives a series of peaks at the signal periodicities (its frequencies and all harmonics). These clean spectra are easily and more reliably identified. For a chaotic trajectory a continuum spectrum without any well-defined peak is expected. The power spectrum and the correlation function are Fourier transforms of each other via the Weiner–Khinchin theorem.[14,15]

E. Numerical results and discussion

We present here some of the results we have obtained applying the above methods. The four explained indicators appear in Fig. 5 for the case of a regular trajectory. We can see that all of them suggest such an interpretation for this case. Note that the value for the energy is very high, $E/m = 2000$ J/kg. As we mentioned above, most of the trajectories are regular for such high values. E/m is a hundred times smaller for the case considered in Fig. 6. The trajectory there turns out to be chaotic. All indicators there suggest such a conclusion. Whereas some of them are perhaps ambiguous, as the power spectrum [Fig. 6(d)], other indicators permit almost no doubt, as the maximum Lyapunov exponent [Fig. 6(b)].

We present in Fig. 3 three Poincaré sections for different values of the energy. In all three cases the solid curves mark the boundary of the allowed region for a given energy. The three graphs are given using the same scale to make comparison easier. We can check the fact that increasing the
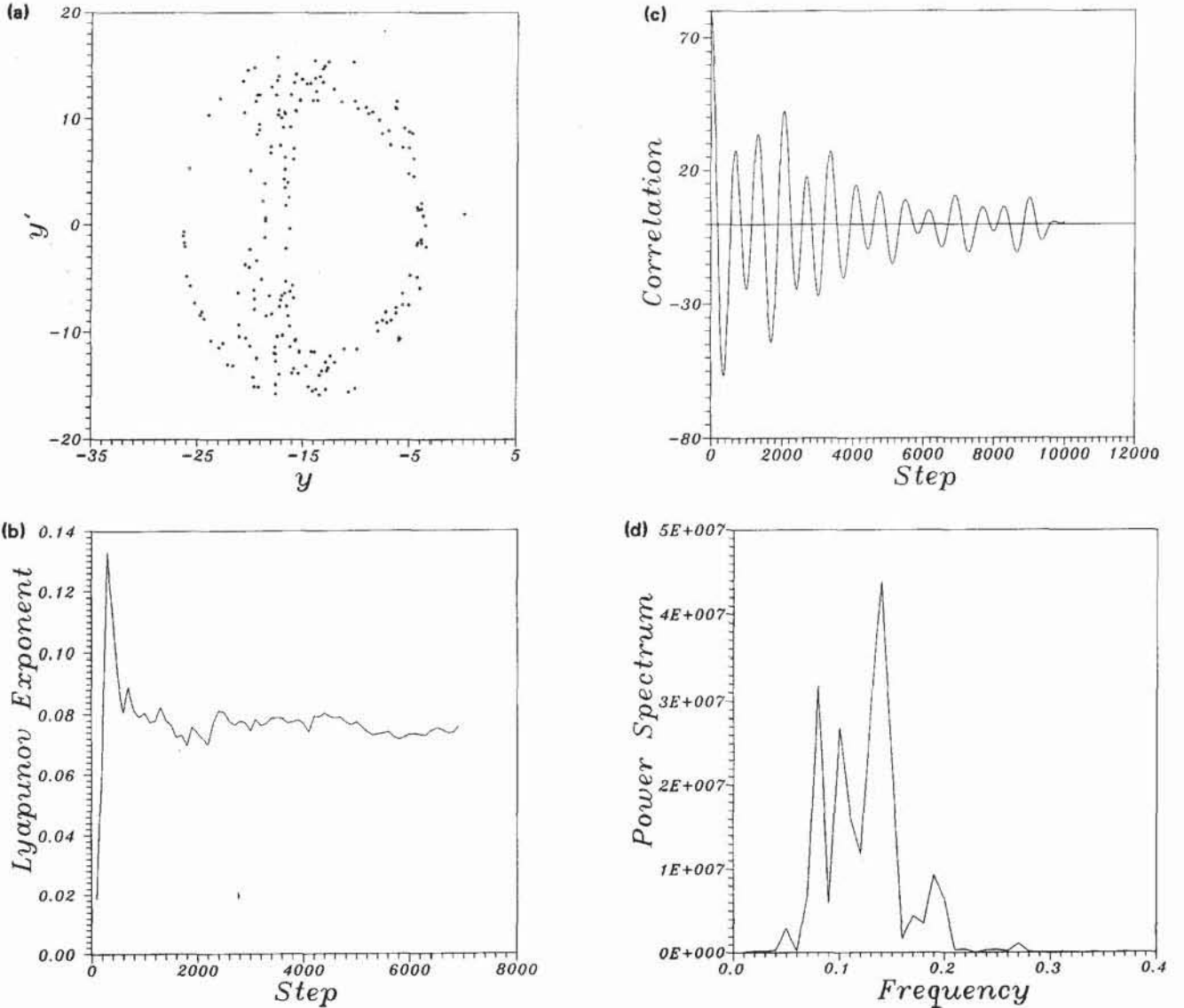

Fig. 6. Same as Fig. 5 but for a trajectory with parameters $E/m = 20$ J/kg, $\omega_m^2 = 2$ s^{-1}, $\lambda = 2$, and initial conditions $x = 5$ m, $y = -5$ m, $\dot{y} = 1$ m/s.

energy from large negative values of E/m means increasing the region of phase space occupied by chaotic trajectories, whereas for large positive values of E/m energy one can see numerically that integrability starts to dominate again.[1] In the last reference some nonnumerical arguments are also used. We have given some other arguments of this kind in a previous section.

V. CONCLUSIONS

We have seen that the elastic pendulum is a physical system which, though simple when compared with others in Nature, features a highly complex dynamics as a result of nonlinearity; there exist chaotic trajectories in its phase space, along with regular ones. Moreover, they seem to form a structure such as those that fit KAM requirements. Our method of arriving at the result is novel, although the result itself[1-4] is not new. Simultaneous study of four different indicators to characterize a system trajectories seems advisable due to the complementary value they have, as was said above. It is specially indicated when computing with modest facilities. Also, the indicators studied have very direct interpretations and may help convey the idea that most systems in Nature are really nonintegrable and therefore possess very complicated patterns of evolution. This perspective can be made more accessible to a wider audience. The elastic pendulum is very suitable for introducing nonlinear dynamics to undergraduate students.

[1] H. N. Núñez-Yépez, A. L. Salas-Brito, C. A. Vargas, and L. Vicente, "Onset of chaos in an extensible pendulum," Phys. Lett. A **145**, 101–105 (1990).

[2] M. G. Olsson, "Why does a mass on a spring sometimes misbehave?," Am. J. Phys. **44**, 1211–1212 (1976).

[3] H. M. Lai, "On the recurrence phenomenon of a resonant spring pendulum," Am. J. Phys. **52**, 219–223 (1984).

[4] Y. Cohen, S. Katz, A. Peres, E. Santo, and R. Yitzhaki, "Stroboscopic views of regular and chaotic orbits," Am. J. Phys. **56**, 1042 (1988).

[5] M. V. Berry, "Regular and irregular motion," in *AIP Conference Proceedings, No. 46,* edited by S. Jorna (American Institute of Physics, New York, 1978), pp. 16–120.

[6] V. I. Arnold, *Mathematical Methods of Classical Mechanics* (Springer-Verlag, New York, 1978), Chap. 10.

[7] A. J. Lichtenberg and M. A. Lieberman, *Regular and Stochastic Motion* (Springer-Verlag, Heidelberg, 1983), pp. 42 ff.

[8] J. M. T. Thompson and H. B. Stewart, *Nonlinear Dynamics and Chaos* (Wiley, New York, 1986).

[9] H. Goldstein, *Classical Mechanics* (Addison-Wesley, Reading, MA, 1959), 2nd ed., pp. 457 ff.

[10] S. E. Koonin, *Computational Physics* (Benjamin Cummings, Menlo Park, CA, 1986), Chap. 4.

[11] G. H. Walker and J. Ford, "Amplitude instability and ergodic behavior for conservative nonlinear oscillator systems," Phys. Rev. A **188**, 416–432 (1969).

[12] G. Benettin and J. M. Strelcyn, "Numerical experiments on the free motion of a point mass moving in a plane convex region; Stochastic transition and entropy," Phys. Rev. A **17**, 773–784 (1978).

[13] G. Benettin, G. L. Galgani, and J. M. Strelcyn, "Kolmogorov entropy and numerical experiments," Phys. Rev. A **14**, 2338–2345 (1976).

[14] A. F. Rañada, "Phenomenology of chaotic motion," in *Methods of Applications of Nonlinear Dynamics,* edited by A. W. Saenz (World Scientific, Singapore, 1988), pp. 1–93.

[15] P. Bergè, Y. Pomeau, and Ch. Vidal, *Order in Chaos* (Aerial, Santa Cruz, CA, 1990).